[7]See, for example, C. Kittel, Introduction to Solid State Physics (John Wiley & Sons, Inc., New York, 1966), 3rd ed., Fig. 27, p. 367.

[8]V. L. Ginzburg and I. D. Landau, Zh. Eksperim. i Teor. Fiz. 20, 1064 (1950).

[9]A. A. Abrikosov, Zh. Eksperim. i Teor. Fiz. 32, 1442 (1957) [translation: Soviet Phys.—JETP 5, 1174 (1957)].

ANISOTROPIC PROPAGATION AND DAMPING OF ION ACOUSTIC WAVES IN A CURRENT-CARRYING PLASMA

Noriyoshi Sato, Akihiko Sasaki, Kazuyuki Aoki, and Yoshisuke Hatta
Department of Electronic Engineering, Tohoku University, Sendai, Japan
(Received 7 September 1967)

Since methods of excitation of ion acoustic waves by an external source with a grid[1] or a small coil[2] were published, propagation and damping of ion acoustic waves were studied most conveniently by a number of authors[1-12] who reported collisional damping,[1,8] Landau damping,[3] viscous damping,[4] existence of geometrical cut-off and no cut-off frequencies,[2,5,7,11] effects of electron contribution at a place far from an exciting region,[6] determination of compression coefficient of electron gas,[9,10] interference,[10] behavior near ion plasma frequency,[12] etc. This Letter reports experimental results and qualitative discussions about anisotropic propagation and damping of ion acoustic waves due to an electric current in a hot-cathode mercury discharge of several hundred milliamperes.

The experimental apparatus is shown in Fig. 1. Wave excitation and detection are done by using two grids with their planes normal to an electric current. One grid is used as an exciter, to which bursts of sinusoidal or continuous sinusoidal waves are applied, and the other as a detector. The frequency of the sinusoidal waves is in the range 10-80 kc/sec, well below the ion plasma frequency (~1 Mc/sec). The experiment is mainly made in the A-G_1 region, because, in the K-G_1 region, the electron thermal velocity is far from drifting-Maxwellian distribution and includes a strong beam especially near the cathode.

A typical example of anisotropic propagation and damping is shown in Fig. 2. The phase velocity (v_p) along the ion drift direction is larger than that along electron drift (against ion drift) direction and the damping along electron drift direction is smaller than that along ion drift direction. The damping seems to follow two slopes along the distance. The larger

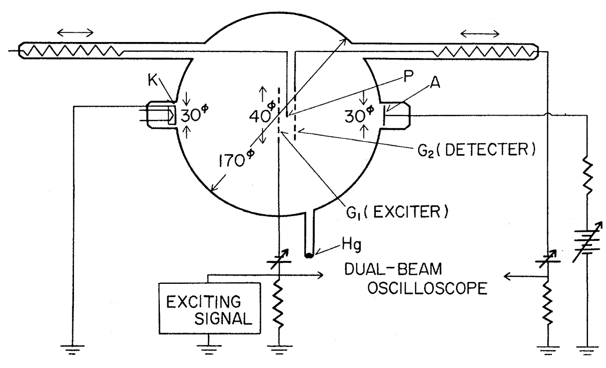

FIG. 1. Experimental apparatus for ion acoustic waves propagating along electron drift. G_2 is used as an exciter and G_1 as detector. A, anode; K, cathode; G_1 and G_2 (movable), grid (10 meshes/in. made of 0.5-mm-diam stainless steel wire); P (movable), probe. All dimensions are in millimeters.

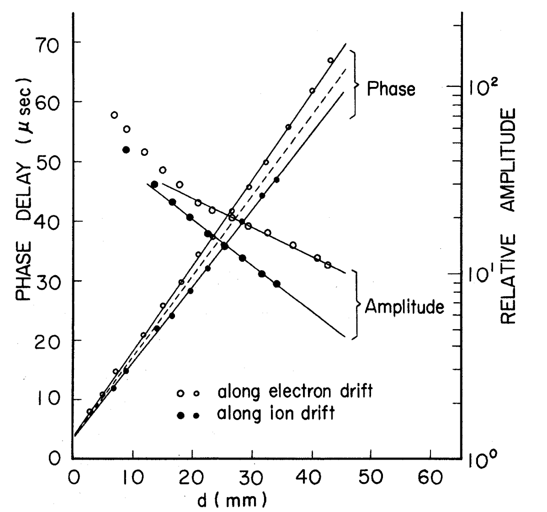

FIG. 2. Phase delay and relative amplitude along electron and ion drifts as a function of the distance (d) from the exciting grid for $f = 45.5$ kc/sec and discharge current = 500 mA. Dashed line ($v_p = 7.34\times10^4$ cm/sec) is obtained from $v_p = (\kappa T_e/m_i)^{1/2}$ and $T_e = 13\,000$°K measured by the Langmuir probe.

slope near the exciting grid may be recognized as verification of Gould's prediction in which the dependence of wave amplitude on the distance (d) from the exciting grid is d^{-1} up to about half a wavelength and, beyond this position, the waves follow exponential decay along the distance. Accordingly, we adopt the smaller slope for determination of the damping distance (δ). It is seen from Fig. 3 that v_p is independent of the frequency (f) and δ^{-1} is inclined to increase linearly with f. The results mentioned above are almost independent of the magnitude of discharge current (100-700 mA) and depend only on its direction.

In a weakly ionized plasma ($T_e \gg T_i$), the dispersion relation of ion acoustic waves[1,13-16] is

$$v_p = c_s \pm V_i, \tag{1}$$

$$\delta^{-1} = \frac{\gamma_i}{2C_s} + \frac{\pi^{3/2}}{\sqrt{2}} f \frac{c_s}{(c_s \pm V_i)^2} \times \left\{ \theta^{3/2} \exp\left(-\frac{\theta}{2}\right) + \rho^{1/2}\left(1 \pm \frac{V_e + V_i}{c_s}\right)\right\}, \tag{2}$$

where $c_s = (\kappa T_e/m_i)^{1/2}$, $\theta = T_e/T_i$, $\rho = m_e/m_i$, the subscripts "e" and "i" refer to electrons and ions, T the temperature, m the mass, V the drift velocity, γ_i the ion-atom collision frequency, and κ the Boltzmann constant. Drifting-Maxwellian velocity distributions and small damping [$(2\pi\delta/\lambda)^2 \gg 1$, λ denotes wavelength] are assumed in Eqs. (1) and (2). The first and second terms on the right-hand side of Eq. (2) denote collisional damping and Landau damping, respectively. In our experiment, $2\pi\delta/\lambda = 4$-12, which justifies the assumption of small damping in deriving Eqs. (1) and (2). The difference of experimental results for the phase velocity along the direction of ion drift with that against ion drift is caused by the Doppler shift due to ion drift as is expected by Eq. (1). $T_e = 12\,500$°K and $V_i = 5\times 10^3$ cm/sec are obtained from v_p along and against ion drift. The dashed line in Fig. 3 is the theoretical value calculated by introducing $T_e = 13\,000$°K obtained from the Langmuir probe method into $v_p = (\kappa T_e/m_i)^{1/2}$. The experimental data for the wave damping result from neither the pure collision damping nor the pure Landau damping, but the combination of these two types of damping. The results for anisotropic damping are believed to

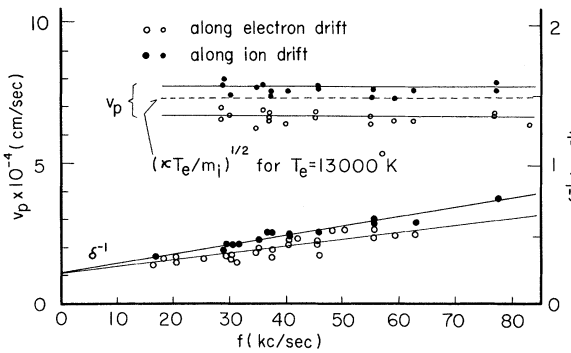

FIG. 3. Phase velocity (v_p) and damping distance (δ) along electron and ion drifts as a function of frequency (f) for discharge current = 500 mA.

be due to the term of electron drift in Eq. (2). It is worthwhile to notice that, according to the experimental results and Eq. (2), we are able to determine the following plasma parameters, i.e., V_e and T_e/T_i from the slopes of δ^{-1} lines and γ_i from the interception of these lines on the ordinate at $f = 0$ kc/sec in Fig. 3. In the present experiment, they are determined as $V_e \sim 1\times 10^6$ cm/sec, $T_e/T_i \sim 11$ ($T_i \sim 1100$°K for $T_e = 12\,500$°K), and $\gamma_i \sim 3\times 10^4$ sec^{-1}. These data on γ_i seem to be too large at the pressure of 1 μ Hg and $T_i \sim 1100$°K, where $\gamma_i \lesssim 1\times 10^4$ sec^{-1} is expected based on an elastic-collision model. This discrepancy may result from the fact that γ_i in our experiment includes not only the ion-atom collisions but also other effective collisions, for example, the collisions with the wall, the ionization collisions, the charge-exchange collisions, the loss of particle momentum from G_1-G_2 region, etc. Referring to Brown's data for various ionized gases,[17] $V_e \sim 1\times 10^6$ cm/sec and $V_i \sim 5\times 10^3$ cm/sec are reasonable values in our experimental conditions ($E \sim 0.01$ V/cm and $P \sim 1$ μ Hg). More details of the study are to be published elsewhere.

[1]Y. Hatta and N. Sato, in Proceedings of the Fifth International Conference on Ionization Phenomena in Gases, Munich, Germany, 1961, edited by H. Maeckner (North-Holland Publishing Company, Amsterdam, The Netherlands, 1962), p. 478.

[2]P. F. Little, in Proceedings of the Fifth International Conference on Ionization Phenomena in Gases, Munich, Germany, 1961 (North-Hollaand Publishing Company, Amsterdam, The Netherlands, 1962), p. 1440; Nature 194, 1137 (1962).

[3]A. Wong, R. W. Motley, and N. D'Angelo, Phys. Rev. 133, A436 (1964).

[4]R. W. Motley and A. Y. Wong, in Proceedings of the Sixth International Conference on Ionization Phenomena in Gases, Paris, France, 1963, edited by P. Hubert (S.E.R.M.A., Paris, France 1964), Vol. 3, p. 133.
[5]P. F. Little and H. G. Jones, Proc. Phys. Soc. (London) 85, 979 (1965).
[6]A. Y. Wong, Phys. Rev. Letters 14, 252 (1965).
[7]P. J. Barrett and P. F. Little, Phys. Rev. Letters 14, 356 (1965).
[8]G. M. Sessler, Phys. Letters 16, 277 (1965).
[9]I. Alexeff and W. D. Jones, Phys. Rev. Letters 15, 286 (1965).
[10]W. D. Jones and I. Alexeff, in Proceedings of the Seventh International Conference on Ionization Phenomena in Gases, Belgrade, 1965 (Gradjevinska Knjiga Publishing House, Beograd, Yugoslavia, 1966).
[11]F. W. Crawford and R. J. Kuhler, in Proceedings of the Seventh International Conference on Ionization Phenomena in Gases, Belgrade, 1965 (Gradjevinska Knjiga Publishing House, Beograd, Yugoslavia, 1966), p. 326.
[12]G. M. Sessler, Phys. Rev. Letters 17, 243 (1966); Phys. Letters 22, 363 (1966).
[13]R. W. Gould, Phys. Rev. 136, A991 (1964).
[14]E. A. Jackson, Phys. Fluids 3, 789 (1960).
[15]G. M. Sessler, Phys. Fluids 7, 90 (1964).
[16]N. Sato and Y. Hatta, J. Phys. Soc. Japan 21, 1801 (1966).
[17]S. C. Brown, Basic Data of Plasma Physics (John Wiley & Sons, Inc., New York, 1959).

ELECTRIC FIELD DEPENDENCE OF OPTICAL-PHONON FREQUENCIES

J. M. Worlock and P. A. Fleury
Bell Telephone Laboratories, Holmdel, New Jersey
(Received 27 September 1967)

In electric-field–induced Raman-scattering experiments on the cubic perovskite $SrTiO_3$, a striking electric field shift and splitting of the "soft" optical phonon mode is observed. Experiments were done at temperatures ranging from 8 to 250°K and for electric fields between 0.2 and 12 kV/cm. We interpret the temperature and electric field dependence of the phonon frequency using Devonshire model of ferroelectricity and the Lyddane-Sachs-Teller relation.

In Cochran's theory of ferroelectricity,[1] soft-phonon modes are of central importance. As the transition temperature is approached from above (in the paraelectric phase) the phonon frequency tends toward zero. We have previously reported studies of the soft-phonon modes in $KTaO_3$[2] and $SrTiO_3$[3] in which an electric field was employed to induce Raman scattering from these odd-parity phonons. In this Letter we report the observation of striking electric field dependence of some optical-phonon frequencies in $SrTiO_3$. In particular, the lowest lying transverse optical phonon has been observed to shift in frequency by 400% and to split into two components polarized parallel and perpendicular to the applied field. Schaufele, Weber, and Silverman[4] have recently observed a small electric-field shift in the soft mode frequency at 77°K.

We have examined the induced Raman scattering at a variety of electric fields (between 0.2 and 12 kV/cm) and at temperatures between 8 and 250°K with the following general results: (1) With very small applied fields the soft-mode frequency varies with temperature from 11 cm^{-1} at 8°K to 85 cm^{-1} at 250°K, in good agreement with the predictions of the Lyddane-Sachs-Teller (LST) relation inserting Weaver's values of the dielectric constant.[5] (2) At low temperatures (<55°K) the spectrum of the field-induced scattering exhibits a field-dependent structure. Figure 1, taken at 8°K, shows that as the field is increased not only does the frequency of the soft mode shift from 11 to 45 cm^{-1}, but also three additional peaks become visible. Those labeled *B* and *C* are identified as components of the soft TO mode, polarized perpendicular and parallel to the applied field, respectively. Peaks *A* and *D* are not components of the soft mode, and appear as well in the intrinsic spectrum of $SrTiO_3$ [see Fig. 1(b)]. (3) The effects of electric field become increasingly strong as the temperature is lowered. This is true for the efficiency of the induced Raman scattering as well as for the shifting and splitting of phonon frequencies. (4) In contrast to the case of $KTaO_3$, we have observed in $SrTiO_3$ induced Raman scattering from the other TO modes at 170 and 550 cm^{-1}. We shall not discuss these results here except to say that these